

SYMMETRIC RELAXATION AROUND INTERSTITIAL 3d IMPURITIES IN SILICON

U. Lindefelt
 Department of Theoretical Physics
 University of Lund
 Sölvegatan 14 A, S-223 62 LUND, Sweden

Alex Zunger
 Solar Energy Research Institute
 Golden, Colorado 80401, U.S.A.

Abstract: EPR studies suggest that most transition atom impurities in silicon occupy the tetrahedral interstitial (TI) site, preserving the T_d symmetry of the host (1). In this paper we will give, within the local-density approximation, a unified description of the electronic structure and "breathing-mode" relaxation of tetrahedral interstitial Cr, Mn, Fe, Co and Ni impurities in bulk silicon.

I. ELECTRONIC STRUCTURE

The electronic structure before relaxation has been calculated self-consistently with the Quasi Band Crystal Field (QBCF) Green's function method (2, 3). Fig. 1 shows the defect energy levels around the band gap introduced by the impurities in their neutral charge state. The numbers in paranthesis give the one-particle occupation consistent with EPR data (maximum spin). Ni is seen not to introduce any gap states, and is thus electrically inactive. Furthermore, since Ni has no partially occupied states, its charge-density has full T_d symmetry and consequently there can be no symmetry-lowering (Jahn-Teller) distortions. For Mn and Cr there are partially filled, electrically active gap states of both e and t_2 symmetry. This is consistent with the empirical fact that

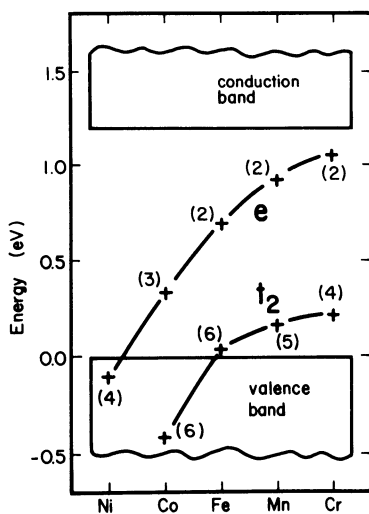


Fig.1. Defect energy levels.

even very small concentrations of the light 3d impurities in silicon considerably shorten the lifetime of free carriers, whereas a much larger contamination by the heavier 3d elements usually can be tolerated. Both the e - and t_2 -states in Fig. 1 are almost 100% d-like in the central cell (CC), defined as the sphere centered at the defect and with a radius equal to the nearest-neighbour distance, 4.44 a.u. In the core region ($\lesssim 1$ a.u.), the wavefunction of the e -state closely resembles that of the atomic 3d state (wavefunction maximum at around $r_m=0.35$ a.u.), with its amplitude at r_m typically reduced by a factor 0.65 compared to the free atom. On the other hand, around 50% of the total charge carried by these states comes from the region outside CC. These states thus share features of both localized and delocalized states, as observed experimentally.

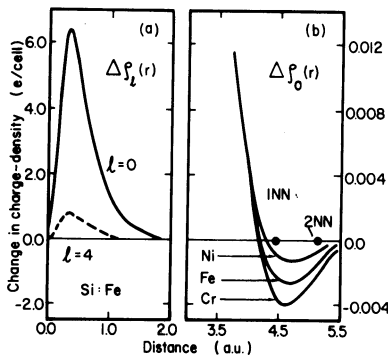


Fig.2. Charge-density perturbation. The impurity is located at the origin.

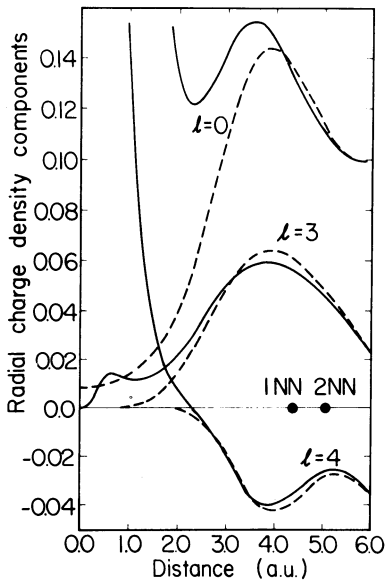


Fig.3. Components of the total charge-density in Si and Si:Fe around TI position.

Fig. 2 shows examples of the radial components $\Delta\rho_\ell(r)$ in a Kubic harmonics expansion of the impurity-induced change in charge-density $\Delta\rho(\vec{r})$:

$$\Delta\rho(\vec{r}) = \sum_\ell \Delta\rho_\ell(r) K_\ell^{a_1}(\vec{r}), \quad K_\ell^{a_1}(1,1,1) \geq 0 \quad (1)$$

The shape of $\Delta\rho_0(r)$ around the first and second nearest neighbours (1NN and 2NN) is depicted in Fig. 2b. As will be seen below, the position of 1NN and 2NN in the antibonding region (negative $\Delta\rho_0(r)$) largely determines the relaxation pattern. The radial components of the full charge-density $\rho(\vec{r})$ are shown in Fig. 3 for the representative case Si:Fe (solid lines) together with the radial components of the host charge-density around the TI site (dashed lines). Apart from the large peaks in the $l=0$ and $l=4$ components, which are both inside the impurity core, there is a rather weak tendency to displace charge from the neighbouring host atoms towards the impurity, and this is effected mainly through the spherically symmetric ($l=0$) component. The 3d impurity is thus essentially filling out the relatively empty TI region without affecting very much the charge density in the rest of the crystal. In this sense, the TI 3d impurities interact weakly with the host.

II. THE LATTICE RELAXATION

When an atom of valence Z_I is placed at an interstitial site \vec{R}_I , it exerts a driving force $\Delta\vec{F}^{(p)}$ on the p :th host atom at \vec{R}_p given by

$$\Delta\vec{F}^{(p)} = \Delta\vec{F}_e^{(p)} + \Delta\vec{F}_{cc}^{(p)} \quad (2)$$

Here the core-core (cc) force is simply

$$\Delta\vec{F}_{cc}^{(p)} = \frac{Z_I Z_H}{|\vec{R}_p - \vec{R}_I|^3} (\vec{R}_p - \vec{R}_I) \quad (3)$$

with Z_H denoting the valence of the host atom. The electronic (e) force can be calculated from the electrostatic Hellmann-Feynman theorem (4), and is for our purposes most conveniently expressed in terms of the projected charge-density $\bar{n}^{(p)}(r)$ through

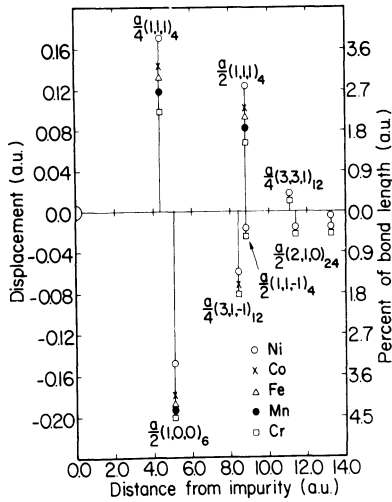


Fig. 4. Displacement of silicon shells $(h,k,l)_N$ containing N atoms.

$$\Delta \bar{F}_e^{(p)} = \int_0^{\infty} [-r^2 \frac{dv_{ps}(r)}{dr}] \bar{n}^{(p)}(r) dr \quad (4)$$

Here $v_{ps}(r)$ denotes the host atom pseudopotential, and the projected density $\bar{n}^{(p)}(r)$ is a vector function, $\bar{n}^{(p)}(r) = (n_x^{(p)}(r), n_y^{(p)}(r), n_z^{(p)}(r))$, whose components are the radial parts of the three partners of the $\ell=1$ term in a Kubic harmonics expansion of $\Delta\rho(\vec{r})$ around the p :th host atom. The restoring forces $\bar{F}_O^{(p)}$ from the host crystal are evaluated from an accurate force-field fitted to phonon spectra (4). The electronic force is evaluated from $\Delta\rho(\vec{r})$ for the undistorted lattice. This means that the basic approximation in the model is that the relaxation-induced change in charge-density is assumed to be the same as in the host crystal (4, 5). This is a good approximation for the weakly interacting impurities considered here. The equilibrium configuration is then evaluated

by requiring that the total force $\bar{F}(\vec{Q}) = \bar{F}_O(\vec{Q}) + \Delta\bar{F}(\vec{Q})$ vanishes at all sites.

Fig. 4 shows the predicted "breathing-mode" distortion. We observe as many as four shells (26 atoms) with a relatively large distortion. Averaging over the impurities, the outward relaxation of the four 1NN is around 0.14 a.u. and the inward relaxation of the six 2NN is around 0.18 a.u. The distance between the two shells has decreased from 0.69 a.u. to 0.37 a.u., i.e. by a factor 2, producing an approximately 10-fold coordinated transition atom. Interestingly, the three bulk disilicide structures, orthorhombic $TiSi_2$, hexagonal $CrSi_2$ and tetragonal $MoSi_2$ are known to avoid the conventional closepacking coordination of 12, and instead assume an approximately 10-fold coordination around the transition atom (6).

The factors controlling the driving forces on the pseudoatoms and hence the relaxation pattern in Fig. 4 are (i) the shape of the pseudopotential and (ii) the position of the atoms in the antibonding area in Fig. 2b. To see this, we have plotted in Fig. 5 the factors in the integrand in Eq. (4). Fig. 5a shows $dv_{ps}(r)/dr$ for the soft-core pseudopotential used here (2) (curve 1), for a hard-core pseudopotential (7) (curve 2) and for a point ion. Fig. 5b shows the magnitude of the projected density for 1NN and 2NN host atoms, constructed from the spherically symmetric component of $\Delta\rho(\vec{r})$ only. The integrand in $\Delta\bar{F}_e$ for the 1NN is shown in Fig. 5c (solid line) and compared to the integrand corresponding to the point-ion potential. Integrating these functions and adding the repulsive $\Delta\bar{F}_{cc}$ results in a driving force $\Delta\bar{F}$ which is slightly attractive for the point ion, but repulsive (i.e. giving the outward distortion) for the pseudo-ion. This difference is thus governed by the different shapes in potentials. For the 2NN the magnitude of the projected density has a negative portion close to the origin (Fig. 5b). When multiplied with $dv_{ps}(r)/dr$, this is seen to lead to an electronic force which is more attractive than for the 1NN. When balanced against $\Delta\bar{F}_{cc}$, this leads to an inward relaxation of the

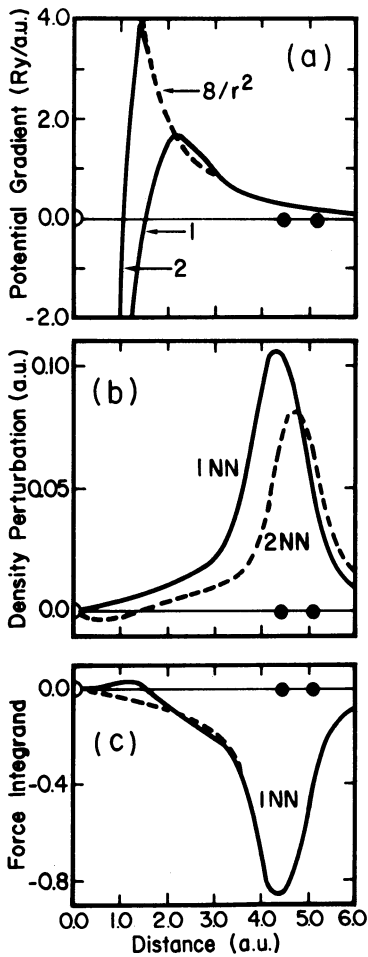


Fig.5. (a) Host pseudopotential gradient. (b) The magnitude of the projected density. (c) The integrand in Eq. (4). The Si atom is at the origin.

2NN. The nodal structure in the projected density for the 2NN, responsible for the different directions of distortion of 1NN and 2NN, is found to be related to the position of the atoms in the antibonding region: the projected density has a node as in Fig. 5b if the atom is located to the right of the minimum in the antibonding region (Fig. 2b), whereas the projected density is nodeless otherwise. The effect of the anisotropic components in $\Delta\rho(\vec{r})$ is to produce a small inward force on both shells. This contribution is, however, not strong enough to reverse the direction of the force on the 1NN. For more distant atoms, $\Delta\vec{F}$ turns out to be negligible, so these atoms have moved only because of the displacement of the first two shells of atoms.

The reason for the relatively large displacement of the fourth shell is that the 4NN atom at $a/2(1,1,1)$, for instance, is directly attached to the 1NN atom at $a/4(1,1,1)$ with a bond in the $(1,1,1)$ -direction, which is also the direction of distortion of the two atoms. This bond is thus compressed only slightly, typically around 1% of the bond length. If only the first two shells of atoms are allowed to relax, this strong coupling between shells leads to a displacement which is about 2/3 of the unconstrained displacement.

REFERENCES

- (1) E.R. Weber, *Appl. Phys.* **A30**, 1 (1983).
- (2) U. Lindefelt and A. Zunger, *Phys. Rev.* **B26**, 846 (1982).
- (3) A. Zunger and U. Lindefelt, *Phys. Rev.* **B26**, 5989 (1982).
- (4) U. Lindefelt, *Phys. Rev.* **B28**, 4510 (1983).
- (5) U. Lindefelt and A. Zunger, to be published.
- (6) A.F. Wells, *Structural Inorganic Chemistry*, fourth edition, (Clarendon, Oxford 1975), p. 789.
- (7) J. Harris and R.O. Jones, *Phys. Rev. Lett.* **41**, 191 (1978).